

## On-off-on Fluorescence Sensor for Detecting Cr<sup>6+</sup> and Ascorbic Acid Using Carbon Dots from Distiller's Grains

Jianan Liu, Chengxiang Wang, Rui Zhu, Hua-Jun Shawn Fan\*

Department of Chemical Engineering, Sichuan University of Science and Engineering, Zigong, China

\*Corresponding Author: fan27713@yahoo.com (Hua-Jun Shawn Fan)

---

### Abstract

Illegal release of hypertoxic Cr<sup>6+</sup> cause huge threat to environment and human health. Thus, constructing low-cost, low-toxic, highly stable and sensitive sensors for Cr<sup>6+</sup> sensing is urgently required. Carbon dots (CDs) have been widely employed for monitoring Fe<sup>3+</sup>, pH, amino acids and antibiotics, but rarely served as probes for Cr<sup>6+</sup> detection. In this research, N-CDs derived from biomass waste (distillers' grains, DGs) were directly obtained by one-step hydrothermal method, which present superior selectivity toward Cr<sup>6+</sup> and exhibit a low Cr<sup>6+</sup> detection limit of 0.1 μM. Based on the characterization and analysis results, a possible detection mechanism based on internal filter effect was proposed for explaining the fluorescence quench by Cr<sup>6+</sup> addition. Notably, the resulted N-CDs+Cr<sup>6+</sup> composite showed a specific affinity toward ascorbic acid (AA) with a 0.2 μM detection limit. In addition, the use of N-CDs as invisible inks in security applications is also explored. In summary, this "on-off-on" N-CDs-based nano-sensor has the advantages of simplicity, convenience, fast response, high selectivity and sensitivity, and has potential for environmental industry.

**Keywords:** carbon dots; Cr<sup>6+</sup>; ascorbic acid; nanosensor; invisible inks; film

---

Date of Submission: 05-03-2024

Date of acceptance: 18-03-2024

---

### I. INTRODUCTION

Over the past few decades, industrial and other anthropogenic processes have constantly released heavy metal ions (Hg<sup>2+</sup>, Pb<sup>2+</sup>, Cd<sup>2+</sup>, As<sup>3+</sup>, Ni<sup>2+</sup>, Cr<sup>6+</sup>, Cu<sup>2+</sup>, Zn<sup>2+</sup>) into the environment [1-3]. Mercury ions can damage the human nervous and immune systems, leading to mental disorders or toxic brain death. Cadmium ions can cause symptoms such as kidney damage or anemia, while lead ions can cause intellectual development disorders and complications such as epilepsy and paralysis in children. Arsenic ions can cause cancer and toxic shock [4-11]. Cr<sup>6+</sup>, one of the hypertoxic metal ions, is acknowledged that it is a strong mutant substance that can induce carcinogenesis when directly discharged into water even at a low density. Thereby, the fast response and in-site determination of Cr<sup>6+</sup> in environmental samples is of great significance [12-17]. Recently, the well-accepted methods for Cr<sup>6+</sup> sensing including chromatography, fluorescence spectrometry, electrochemical analysis and atomic absorption spectrometry have been well documented. Nevertheless, these strategies are still troubled by the complex process of sample pretreatment and expensive equipment [18-20]. Therefore, a highly sensitive and low-cost fluorescent platform for Cr<sup>6+</sup> sensing is urgently required. However, some studies have shown that ascorbic acid (AA) may provide a certain degree of protection against the toxicity of chromium ions. AA is an important vitamin in human diet and has been used for the prevention and treatment of common cold, mental illness, cancer, and AIDS [21]. Among the various methods for detecting AA, fluorescence detection has been widely studied due to its low cost, simplicity, speed, and high sensitivity [22]. In recent years, researchers had developed multiple sensing platforms. For example, Laboratory et al. synthesized compatible silver nanoparticles using flower extract of *Plumeria* as raw material, and the detection line for Cr<sup>6+</sup> is as low as 95 ± 2 pM [23]. Guo et al. synthesized bovine serum albumin stabled gold nanoparticles as detection probes for Cr<sup>6+</sup> with a detection limit down to 120 nM [24]. Tian et al. developed an intelligent hydrogel grating detector, which realized real-times detection of Cr<sup>6+</sup> with a detection limit 9 M in water. Marchesi et al. reported Tb<sup>3+</sup> and Eu<sup>3+</sup> ions were encapsulated in the inorganic layers of a synthetic saponite clay as a sensor for Cr<sup>6+</sup> detection. Sofia et al. have designed a new microporous metal-organic framework with sensitive response to Cr<sup>6+</sup> ions, and the detection limit was 4 ppb [25-27]. However, these sensors and detection methods still have some problems. For example, the detection limit of some detection methods is high, and the preparation method of sensing materials is complicated. Some testing equipment is not portable, the test results are not real-time. Therefore, it is necessary and challenging to design and develop new sensing platforms and methods that are portable, easy to operate, highly selective and highly sensitive.

Carbon dots (CDs), 0-D carbon nanomaterial, has drawn considerable attention due to its low cost, low toxicity, good biocompatibility and high photochemical stability [29-30]. Benefitting from these merits, great efforts have been devoted to developing CDs-based sensors for metal ions ( $\text{Hg}^{2+}$ ,  $\text{As}^{3+}$ ,  $\text{Pb}^{2+}$ ,  $\text{Fe}^{3+}$ ,  $\text{Cu}^{2+}$ ,  $\text{Al}^{3+}$ ,  $\text{Zn}^{2+}$ ), as well as molecules such as Amino acid (Alanine, Isoleucine, Leucine, Valine, Tryptophan), ciprofloxacin, glutathione, dopamine and nitrite [31-38]. However, these probes were rarely sensitive for  $\text{Cr}^{6+}$  and most of them were prepared from commercial resource. In contrast, biomass/biomass waste derived CDs are more attractive and deserve more interest input. For example, Bandi et al. successfully synthesized carbon dots (CDs) using waste cigarette butts as the precursor material. The obtained CDs exhibit blue fluorescence and good stability, with a detection limit as low as  $0.13 \mu\text{M}$  for  $\text{Fe}^{3+}$  [39]. Rao and colleagues used Cinnamomum plants hydrothermal method to prepare CDs with sensitive response to  $\text{Al}^{3+}$  in the concentration range of  $0.2 - 100 \mu\text{M}$ , and the detection limit was as low as  $0.73 \mu\text{M}$  [40]. Boruah used sugarcane bagasse as a raw material for the preparation of probes for the detection of  $\text{F}^-$  with a detection limit of  $0.348 \mu\text{M}$  [41]. Nevertheless, finding an environmentally friendly and easily available carbon source are always the goal pursued by researchers. Recently, a large number of biomass waste Distillers Grains (DGs) have caused a lot of resource waste and environmental pollution [42]. DGs are a by-product of the brewing industry, which is rich in a lot of nutrients such as crude fiber, crude protein, non-nitrogen extract, amino acids and various vitamins and other bioactive substances [43]. If it is not dealt with in time, it will deteriorate and seriously pollute the surrounding environment. The annual output of Chinese DGs is as high as 72.49 million tons, most of them are used for feed preparation, edible fungus culture, anaerobic fermentation biogas recovery of DGs and so on [44]. Interestingly, from another point of view, DGs is a good carbon source for preparing fluorescent CDs, which provides a new idea for the recycling of biomass waste. But only a few efforts were made in this regard. Nkeumaleu et al. studied a method of synthesizing carbon dots from distiller's grains for the detection of  $\text{Cu}^{2+}$  [45]. Kazak et al. reported a carbon material with a specific surface area of up to ( $189 \text{ m}^2/\text{g}$ ) synthesized from DGs for adsorption of Victoria Blue B [46]. Recently, Man et al. have reported the synthesis of carbon dots from DGs and their application for fluorescence detection of  $\text{Fe}^{3+}$  [47]. At present, there is no evidence of using DGs as a carbon source to produce carbon dots for detecting  $\text{Cr}^{6+}$  and AA.

In this study, we explored the use of DGs as source material for the production of highly fluorescent N-doped CDs (N-CDs). The N-CDs were systematically characterized by various analytical techniques, and their N-CDs was synthesized by one-step hydrothermal method with ethylenediamine as surface passivating agent. The stability of N-CDs under high ionic strength, pH, temperature, storage, and continuous irradiation conditions was evaluated. N-CDs exhibited bright and stable fluorescence in aqueous solution, with a quantum yield of 23%. Using N-CDs as an "on-off-on" fluorescence probe, the detection of  $\text{Cr}^{6+}$  and ascorbic acid (AA) showed high selectivity and sensitivity, with determined detection limits and response ranges (The limit of detection (LOD) is  $0.1 \mu\text{M}$  and  $0.2 \mu\text{M}$ ) for  $\text{Cr}^{6+}$  and AA detection. In addition, N-CDs also showed good light stability and great water solubility after 30 days. Without further functional modification, N-CDs can be directly used as a fast, highly selective and highly sensitive  $\text{Cr}^{6+}$  detection sensor and an "on-off-on" fluorescence sensor for AA. Furthermore, we have prepared fluorescent polymer films by incorporating N-CDs into polyvinyl alcohol (PVA). Also these N-CDs were applied as invisible ink for security applications.

### 1.1.1 Material

$\text{Fe}(\text{NO}_3)_3$ ,  $\text{Fe}(\text{NO}_3)_2$ ,  $\text{Cu}(\text{NO}_3)_2$ ,  $\text{Mg}(\text{NO}_3)_2$ ,  $\text{Ni}(\text{NO}_3)_2$ ,  $\text{KNO}_3$ ,  $\text{NaNO}_3$ ,  $\text{Co}(\text{NO}_3)_2$ ,  $\text{Cd}(\text{NO}_3)_2$ ,  $\text{Zn}(\text{NO}_3)_2$ ,  $\text{AgNO}_3$ ,  $\text{Pb}(\text{NO}_3)_2$ ,  $\text{Al}(\text{NO}_3)_3$ ,  $\text{Ca}(\text{NO}_3)_2$ ,  $\text{K}_2\text{Cr}_2\text{O}_7$ , phosphate buffer pH 7.2, PVA (Mw 31,000–50,000), AA, Gly, Glu, Lys, L-ser, L-lys, GSH, Phe were obtained from Shanghai Aladdin Bio-Chem Technology Co., Ltd. Distiller's grains from Sichuan Yibin Baijiu Factory. Deionized water was used throughout the experiment as the solvent. The solution of  $\text{Cr}^{6+}$  was prepared from  $\text{K}_2\text{Cr}_2\text{O}_7$ . The solutions of metal ions were prepared from their nitrate salts.

### 1.1.2 Fabrication of N-CDs

Here, we report the preparation of N-CDs from DGs by a simple hydrothermal method. The method of preparing N-CDs from DGs was shown in Scheme 1. Typically, 0.50 g DGs and 200  $\mu\text{L}$  Ethylenediamine (EDA) were dispersed in 15 mL Deionized water. The solution was centrifuged for 10 minutes to remove insoluble substances, then transferred to a Teflonlined autoclave where it is heated at  $200^\circ\text{C}$  for 5 hours. The naturally cooled solution was centrifuged at 8000 rpm for 10 minutes to remove large particles. Then freeze-dried into a powder and stored in a refrigerator at  $4^\circ\text{C}$  for subsequent use.

### 1.1.3 Characterization and apparatus

The structural properties and elemental composition of N-CDs were characterized by the following instruments. The transmission electron microscope (TEM) was performed by JEM-1400 Flash analyzer. Raman spectra were tested by using the Horiba scientific-LabRAM HRevoluion (Japan). The powder X-ray diffraction (XRD) pattern was investigated from Bruker D8 Advance X-ray diffractometer. The Raman spectra was measured Thermo Fisher DXR spectroscopy. The Fourier transform infrared (FTIR) spectroscopy was acquired using Bruker Tensor spectrometer. The X-ray photoelectron spectroscopy (XPS) data was performed by PHI-5000VersaProbeIII spectrophotometer. The optical properties of N-CDs were explained by the characterization results of such instrumentation. The ultraviolet-visible (UV-Vis) absorption spectra were revealed through Hitachi U-2900 spectrophotometer. The fluorescence spectroscopy was presented by Horiba FluoroMax 4 fluorescence spectrometer.

### 1.1.4 Fluorescence detection of Cr<sup>6+</sup> and AA

Solutions of all metal ions used in this experiment are prepared from corresponding salts in DD water. At room temperature, 1 mL of Deionized water is added to 1 mL of N-CDs aqueous solution(0.1 mg/mL), the emission spectra of this sample are recorded at an excitation wavelength of 340 nm, and the emission intensity at 430 nm is denoted as F0. Prepare solutions of Cd<sup>2+</sup>, Ca<sup>2+</sup>, La<sup>2+</sup>, Fe<sup>2+</sup>, Cu<sup>2+</sup>, Al<sup>3+</sup>, Li<sup>+</sup>, Ba<sup>2+</sup>, Zn<sup>2+</sup>, K<sup>+</sup>, Co<sup>2+</sup>, Mg<sup>2+</sup>, Ce<sup>3+</sup>, Na<sup>+</sup>, and Fe<sup>3+</sup> with a concentration of 1 mM. Add 200 μL of N-CDs solution and 200 μL of ion solution respectively to a 2 mL centrifuge tube, and then add 1600 μL of Deionized water to obtain a mixed solution with a uniform metal ion concentration of 1 mM. Record the fluorescence spectrum of the liquid at room temperature at an excitation wavelength of 340nm and record the emission intensity as F. A similar procedure was followed for the quantitative determination of Cr<sup>6+</sup>. In typical measurements, 1mL of N-CDs solution is mixed with 1mL of different concentrations of Cr<sup>6+</sup> solution, and the fluorescence intensity under 340nm excitation is recorded. Prepare 0.2 mL of the above mixture of N-CDs solution and Cr<sup>6+</sup> solution was used with 2 mL of 1 mM of various ions (AA, Gly, Glu, Lys, L-ser, L-eyes, GSH, Phe) were mixed and shaken well. The fluorescence spectra of liquids were recorded at room temperature at excitation wavelength of 340 nm.

### 1.1.5 Calculation of fluorescence QY

The QY is calculated using the following equation:

$$\varphi_S = \varphi_R \frac{I_S A_R \eta_S^2}{I_R A_S \eta_R^2}$$

$\varphi$  stands for QY, I mean the integrated area of the fluorescence intensity, A is the absorbance,  $\eta$  denotes the refractive index of the solvent, and S and R represent the sample and reference, respectively.

### 1.1.6 Preparation of N-CDs/PVA anti-counterfeiting film

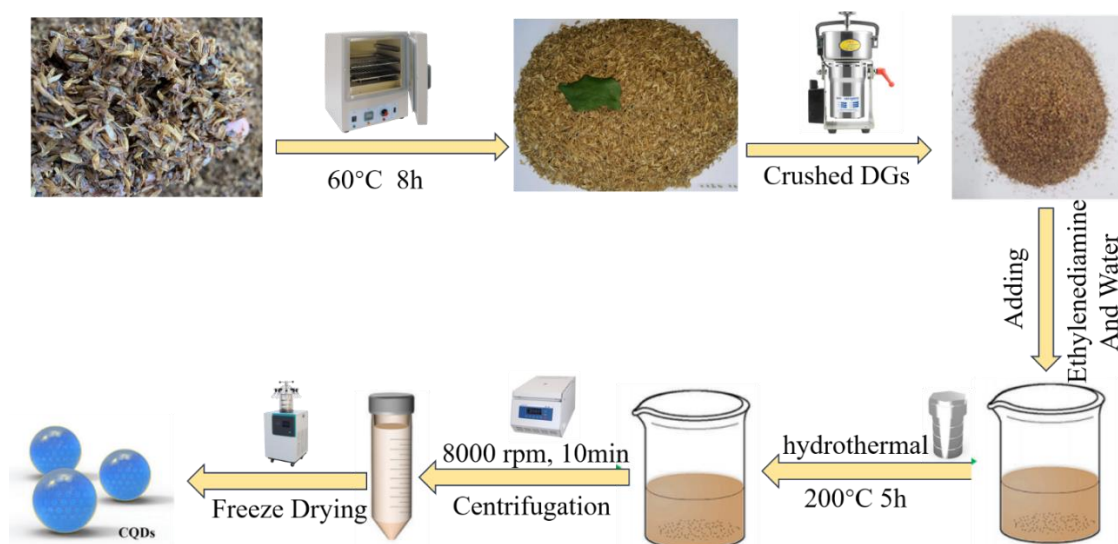
1.2 g PVA was added into 18 mL Deionized water, then the mixture was heated to 80°C. After the PVA was dissolved in water, 4.0 mg/mL N-CDs was added to the PVA solution under vigorous stirring. The obtained solution was used for preparing flexible-transparent N-CDs/PVA composite film by using our home-made instrument.

### 1.1.7 Stern Volmer plots and determination of limit of detection.

The experimental PL data were fitted using the Stern Volmer equation:

$$F_0/F = K_{SV} [Q] + 1$$

where F<sub>0</sub> is the PL intensity of N-CDs in water, F is the PL intensity in the presence of the contaminant, K<sub>SV</sub> is the Stern-Volmer quenching constant (slope of the concentration dependent response), and Q is the quencher concentration. Then, the limit of detection (LOD) was calculated using the formula 3σ/K (σ is standard deviation and K is the slope of the calibration plot)



**Scheme 1. Schematic Representation of the Synthesis of Fluorescent N-CDs form DGs**

## II. RESULT AND DISCUSSION

The results obtained are as discussed below

### 2.1 Morphology and Structure of N-CDs.

To better evaluate the morphology, structural and chemical composition of N-CDs influencing on the optical properties, it was characterized by TEM, AFM, XRD, Raman, FT-IR, XPS and other techniques. TEM images (Fig. 1a) shows that the N-CDs is dispersed uniformly and presented in quasi-spherical morphology [48]. The size of the as-prepared N-CDs is distributed in the range from 2.5 to 5 nm, with an average size of 3.5 nm (inset of Fig. 1a). By the high-resolution TEM (HRTEM) (Fig. 1b), the carbon core of the N-CDs has distinct lattice stripes of 0.21 nm which resembles the 100 facets of graphite [49-51]. In addition, the AFM image of N-CDs (Fig. 1c and Fig. 1g) was also recorded, and it can be seen that the height of the N-CDs was around 4 nm with a multi-layerstacked structure [52]. The microcosmic structure of N-CDs was further investigated by XRD and a sharp diffraction peak near the center at  $2\theta = 22.4^\circ$  belongs to the (100) crystalline plane of graphite which indirectly supports the results obtained in the HRTEM image [53]. Two distinct Raman spectral bands were detected, as shown in Fig 1e, with the D band and G band. The D band represents the disordered carbon and indicates a defect in the structure of N-CDs, which is caused by the doping of other atoms such as N and O elements and could regulate the fluorescence performance of N-CDs [54]. The G band represents the graphitized ordered carbon structure peak. The ID/IG ratio is greater than 1, which indicates that more defect sites appeared in the N-CDs structure [55]. The surface functional groups of CDs were characterized through Fourier transform infrared (FTIR) spectroscopy. The broad vibrational band in the range of  $3600\text{--}3400\text{ cm}^{-1}$  can be attributed to the stretching vibrations of N-H and O-H. A strong band at  $2944\text{ cm}^{-1}$  is attributed to the stretching modes of C-H stretching vibration. The peaks at  $1740\text{ cm}^{-1}$  C=C and  $1643\text{ cm}^{-1}$  are ascribed to the C=O. the peak at  $1470\text{ cm}^{-1}$  implies the presence of C-N, and there is also a peak at  $1093\text{ cm}^{-1}$  which belongs to C-O bond [56-58]. These functional groups improve the hydrophilicity and stability of the N-CDs in an aqueous system, which is conducive to the applications of N-CDs in the area of fluorescence probes.

To further validate the above characterization results, The XPS spectra of the N-CDs show three peaks at 285.0, 398.8, and 530.6 eV, which are assigned to the C 1s, N 1s, and O 1s, as depicted in Fig. 2. In addition, the high-resolution XPS spectra of C 1s (Fig. 2a) can be well deconvoluted into four surface components, corresponding to sp<sup>2</sup> (C=C/C-C) at binding energy of 284.8 eV, C-N at 285.4 eV, C-O at 286.2 eV, and C=O at 287.9 eV. The spectra of O1s at 532.4 eV and 530.6 eV represent the peaks at C-O and C=O, respectively (Fig. 2b). The spectrum of N 1s (Fi. 2c) exhibits three peaks at 399.1 and 400.8 eV, related to pyrrolic-N and amino groups, respectively [59-62]. That indicates that N was doped into the graphite structure in the N-CDs. The surface components of the N-CDs determined by the XPS are in good agreement with FT-IR results.

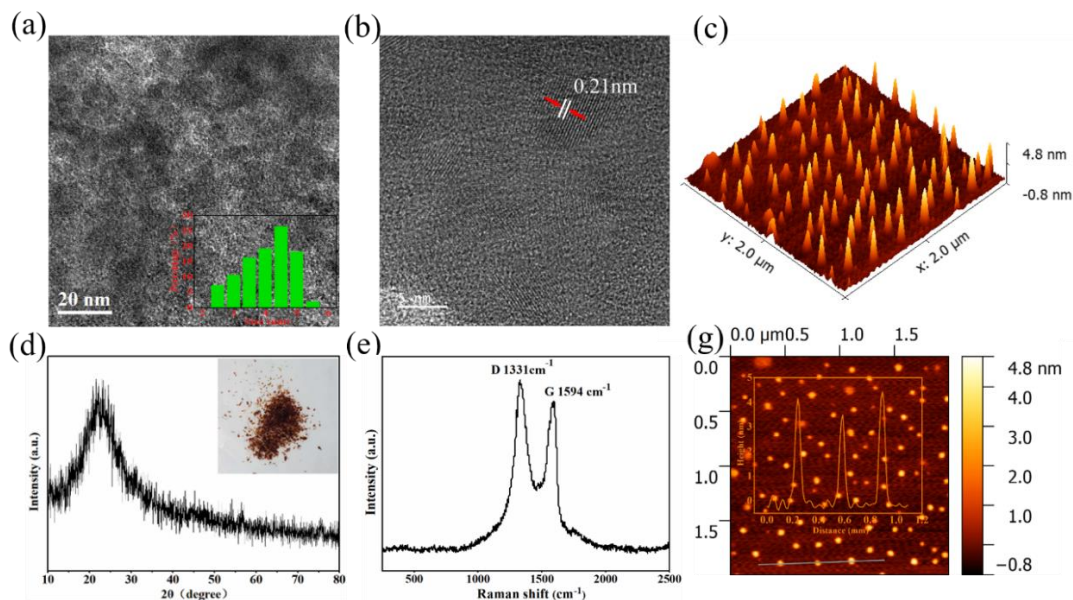


Figure 1: (a) TEM image, particle size distribution (insets). (b) HR-TEM images. (c) AFM images of N-CDs. (d) XRD pattern. (e) Raman spectra. (g) AFM images of N-CDs.

## 2.2 Fluorescence Performance of CQDs.

The optical properties of the N-CDs were investigated (Fig. 2). The UV-vis absorption spectra displayed two absorption regions of the three N-CDs. Fig. 2e shows the UV-vis absorption and photoluminescent spectra of N-CDs under different excitation wavelengths. The absorption spectrum displays two resolved bands around 260 and 330 nm, which can be ascribed to the  $\pi-\pi^*$  transition of carbonic core center and  $n-\pi^*$  transition of heteroatomic surface functionalities or molecule center, respectively [63].

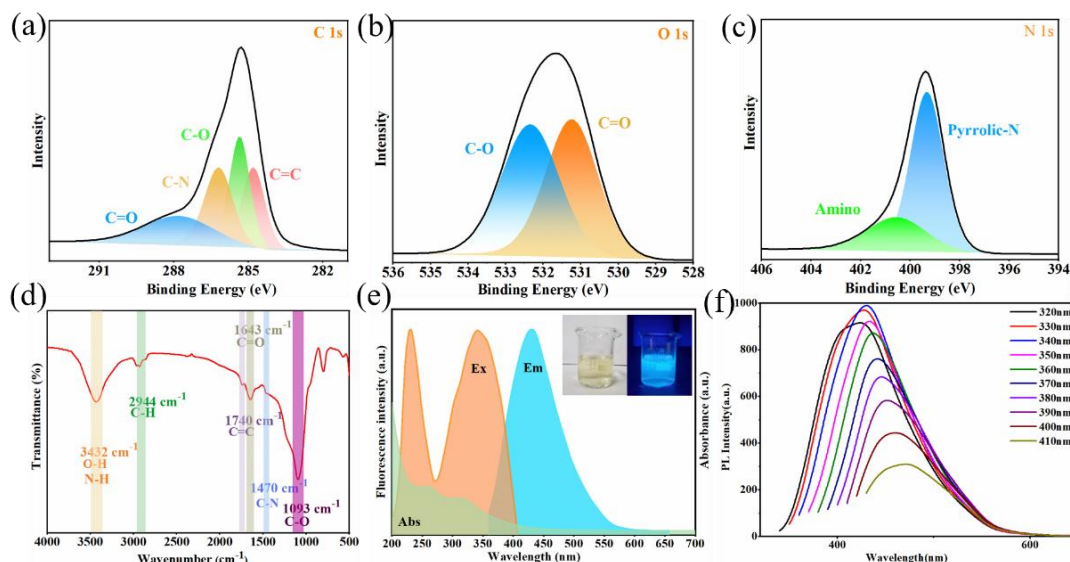
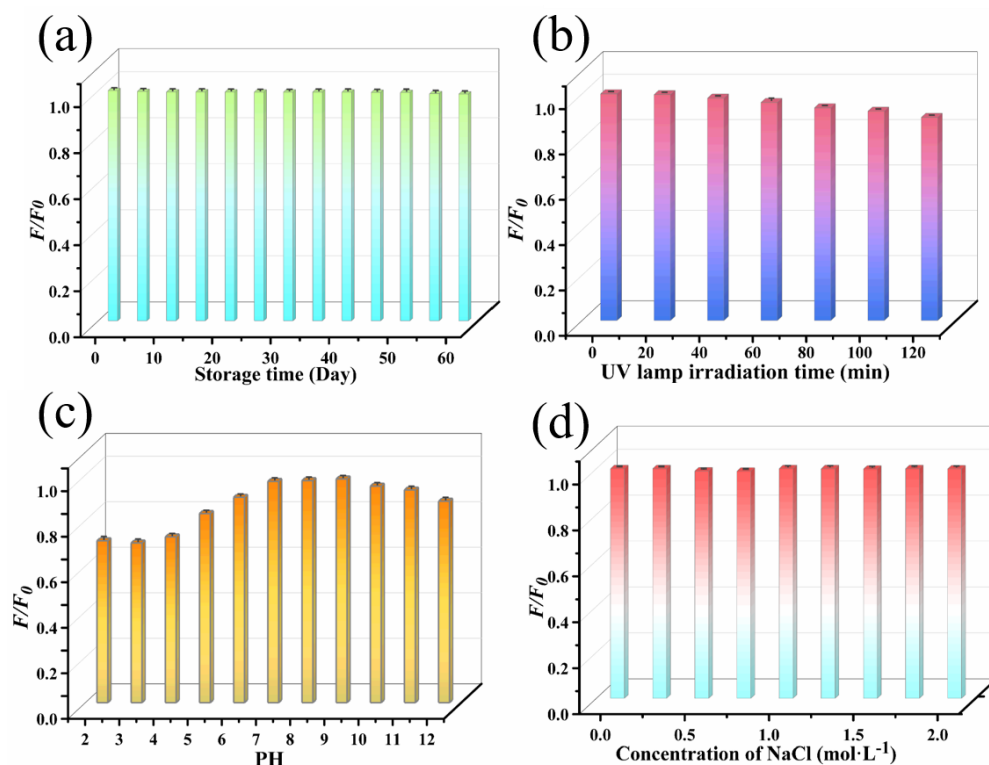


Figure 2: High-resolution spectra of (a) C 1s, (b) N 1s, and (c) S 2p peaks. (d) FT-IR spectra. (e) UV-Vis, best excitation and emission fluorescence spectra. (f) Emission spectra at different wavelengths of excitation.

N-CDs aqueous solution glows bright blue under 365 nm UV light, and it appeared transparent and pale yellow under daylight (inset of Fig. 2e). The corresponding excitation spectrum shows two peaks, which can be ascribed to core and surface excitations. Like most of the fluorescent CDs, N-CDs also exhibited excitation

tunable emission behavior. A steady increase in  $\lambda_{ex}$  from 320 to 410 nm resulted in a red shift in the emission peak position along with a concurrent first increase and then decrease in the emission intensity (Fig. 3f). The maximum emission peak centered at 430 nm was observed under the excitation of 340 nm with a large stokes shift of 90 nm.[64] As a result, an aqueous solution of CDs fluoresces blue under a 365 nm UV lamp (see illustration in Figure 3e). The quality of carbon points is closely related to raw materials, synthesis methods and surface chemical properties involved. Using quinine sulfate (0.1M H<sub>2</sub>SO<sub>4</sub> as solvent, QY = 0.54) as reference, the QY of N-CDs is 23% by slope method. Visible excitation and emission, relatively high QY, and biomass waste as raw materials indicate that N-doped CDs have great application potential in analyte sensing.

Outstanding probes should demonstrate excellent fluorescence stability under diverse conditions. As evident in the Fig. 3a, the fluorescence intensity of N-CDs is virtually constant over a period of up to 60 days. The N-CDs maintains excellent fluorescence emission without interference for up to 120 min when irradiated with either 365 nm UV lamp (Fig. 3b). As shown in Figure 6, changing the pH of the solution can lead to a change in emission intensity. Within the pH range of 6-11, no significant changes in recorded emission intensity were observed, highlighting the advantageous characteristics of fluorescent probes in complex biological systems and practical applications. Additionally, to assess the adaptability of N-CDs in diverse biological environments, it was observed that fluorescence loss did not exceed 5% of its initial value in 0.01–2.0 M NaCl solutions, indicating its exceptional resistance to ionic interference (Fig. 3d). The above experiment highlights the excellent stability of N-CDs fluorescence imaging.



**Figure 3: Effect of (a) storage time (b) UV irradiation (c) PH and (d) ionic strength on fluorescence intensity of N-CDs .**

### 2.3 N-CDs Fluorescent Sensors for Detecting Cr<sup>6+</sup> Ions and AA.

Due to the excellent optical properties of N-CDs, we are encouraged to further study the potential sensing applications of N-CDs. According to previous reports, the surface functional groups of CDs can selectively interact with metal ions and produce fluorescence changes; thus, we have studied the fluorescence response of N-CDs toward various biologically and environmentally important metal ions, such as Cd<sup>2+</sup>, Ca<sup>2+</sup>, La<sup>2+</sup>, Fe<sup>2+</sup>, Cu<sup>2+</sup>, Al<sup>3+</sup>, Li<sup>+</sup>, Ba<sup>2+</sup>, Zn<sup>2+</sup>, K<sup>+</sup>, Co<sup>2+</sup>, Mg<sup>2+</sup>, Ce<sup>3+</sup>, Na<sup>+</sup>, Fe<sup>3+</sup> shown in Fig. 4c, among all ions, only Fe<sup>3+</sup> caused a severe decline in the PL intensity, which unveiled the applicability of N-CDs as highly selective turn-off fluorescent probes for Cr<sup>6+</sup> detection. The method has good specificity for Cr<sup>6+</sup>, and can meet the high selectivity requirements for Cr<sup>6+</sup> in practical applications. Finally, Fig. 4b presents the relationship between the

concentration of  $\text{Cr}^{6+}$  and the fluorescence intensity of N-CDs, with a linear response in the range of 0.01–200  $\mu\text{M}$  ( $R^2 = 0.99534$ ) and the LOD of 0.10  $\mu\text{M}$  ( $S/N=3$ ), which was much lower than the maximum concentration (0.96  $\mu\text{M}$ ) of  $\text{Cr}^{6+}$  in drinking water permitted by the WHO [65]. This means that our IFE-based fluorescence method is sensitive enough to monitor the concentration of  $\text{Cr}^{6+}$  in drinking water. This N-CDs based “turn-off” fluorescent probe via IFE provides obvious advantages of simplicity, convenience, and rapid implementation and thus has potential application for the detection of  $\text{Cr}^{6+}$  in the environmental industry.

Since  $\text{Cr}^{6+}$  and AA can react under very mild conditions, the reduction reaction of  $\text{Cr}^{6+}$  in the presence of AA has received extensive attention. In this work, AA had the function of turning on the fluorescence signal of N-CDs+ $\text{Cr}^{6+}$  in Fig. 6d. Therefore, under the identical conditions, we explored the effects of some reducing agents and vitamins (AA, Gly, Glu, Lys, L-ser, L-lys, GSH, Phe) on the fluorescence signal of CDs+ $\text{Cr}^{6+}$  system. From Figure 5f, it can be seen that AA has specificity in restoring fluorescence, because AA reduces  $\text{Cr}^{6+}$  to a low valence state, it can eliminate the IFE effect of N-CDs+ $\text{Cr}^{6+}$ , thereby restoring the fluorescence of N-CDs [66-68]. For this reason, the N-CD+ $\text{Cr}^{6+}$  system could behave as a “turn-on” fluorescent sensor for detection of AA. As shown in Figure 5d, the fluorescence of the N-CD+ $\text{Cr}^{6+}$  and AA mixture was enhanced gradually with increasing concentration of AA. A good linear relationship of fluorescence intensity and AA concentration is observed from 0.01 to 125 $\mu\text{M}$  (Fig. 6e), with a linear equation of  $I = 0.02193 [\text{AA}] (\mu\text{mol/L}) + 1.15513$  ( $R = 0.997$ ). The corresponding detection limits were 0.2 $\mu\text{M}$ . Generally, the above results provide a sensitive and broad detection range for the determination of AA. This N-CD+ $\text{Cr}^{6+}$  based “turn-on” fluorescent nanosensor provides obvious advantages of simplicity, convenience, and rapid implementation.

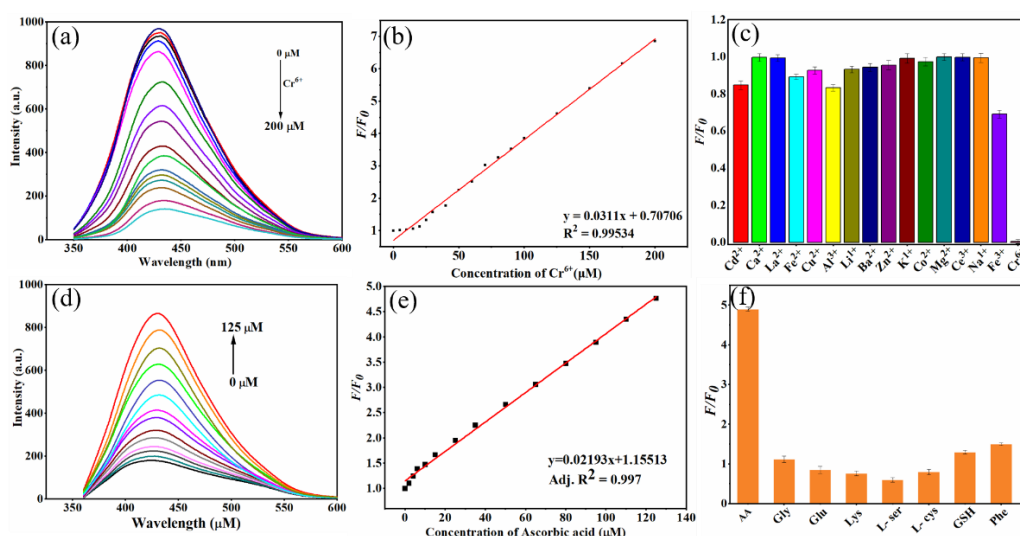


**Fig.4:** (a) Fluorescence intensity response of CDs with increasing concentration of  $\text{Cr}^{6+}$ . (b) Relationship between  $F/F_0$  and the concentration of  $\text{Cr}^{6+}$  ions in the range of 0–200 $\mu\text{M}$ . (c) Fluorescence response ( $F/F_0$ ) of CDs toward various metal ions. (d) Fluorescence intensity response of CDs+ $\text{Cr}^{6+}$  with increasing concentration of AA. (e) Relationship between  $F/F_0$  and the concentration of AA in the range of 0.01–125 $\mu\text{M}$ . (f) Fluorescence response ( $F/F_0$ ) of CDs+ $\text{Cr}^{6+}$  system toward various commonly interfering species.

## 2.4 Fluorescent Ink and Polymer.

In this work, the resulting N-CDs have unique properties, including excellent thermal and light stability as well as good visible light region transparency, which makes them suitable candidates for fluorescent ink applications. To explore this, we filled the N-CDs water solution with a sketch pen and wrote some text on commercial filter paper. We can clearly see the SUSE logo under 365 UV irradiation from Fig. 6a. As shown in Fig. 6b, the word "SUSE" is clearly visible under ultraviolet light (showing blue fluorescence). It is worth mentioning that even after 30 days (when stored under environmental conditions), the information on the filter paper remains consistent and can be reproduced. N-CD has high biocompatibility and can be safely used as an ink pad to form human fingerprints that do not contaminate fingers. (Fig. 6c) These observations indicate that N-CD can be used as stealth ink to load important information for secret communication and has enormous potential in anti fraud applications [70].

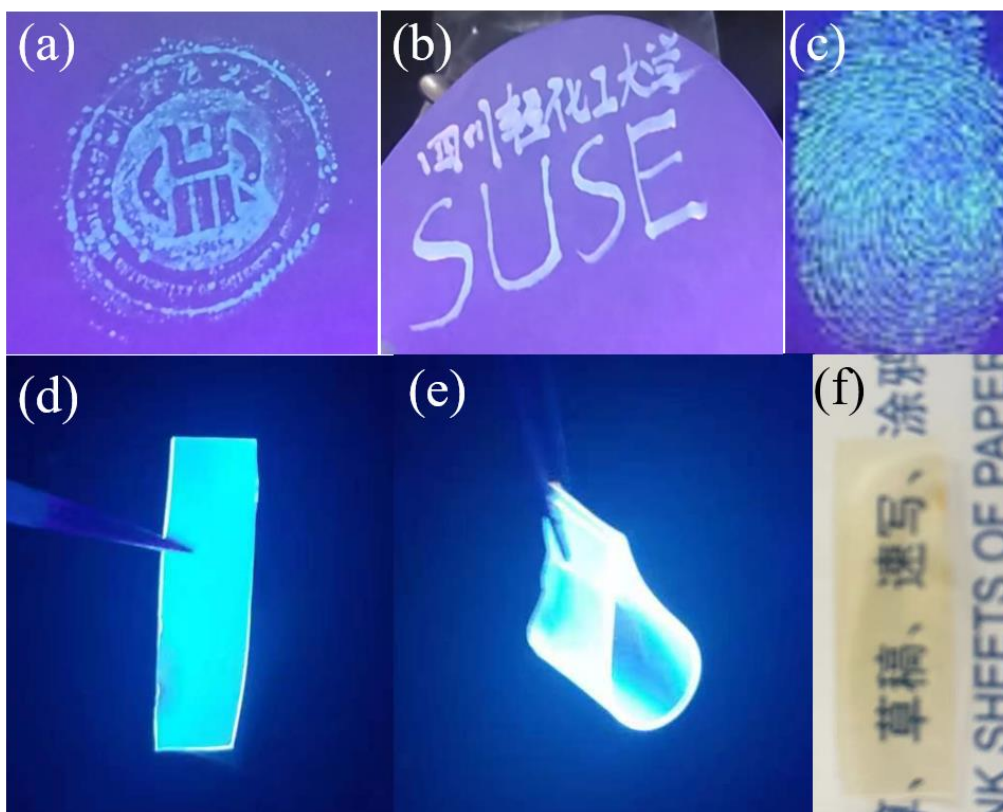


**Figure 3: Information loaded on commercial filter paper using N-CDs invisible ink under 365 nm UV light. (a) N-CDs as fluorescent ink for seals, (b) N-CDs as confidential ink for writing on filter paper, (c) N-CDs formed fingerprints under 365 nm UV light. N-CDs/PVA film (d, e) under 365 nm UV light, (f) under daylight.**

### III. CONCLUSION

In summary, we have successfully demonstrated a simple one-step hydrothermal method for the production of highly fluorescent ( $QY = 23\%$ ) N-doped N-CDs from DGs for the first time. Moderate reaction conditions, using biomass waste materials as starting material, and multifunctional nature of the formed products (N-CDs) make our method economical and scalable. The as-produced N-CDs were well characterized and explored for multiple applications. Bright and stable fluorescence coupled with high biocompatibility made N-CDs a potential candidate for fluorescence detection sensors. They were successfully applied as “on–off–on” fluorescent probe for the sequential detection of  $Cr^{6+}$  and AA. N-CDs were further employed as invisible ink for loading data and forming fingerprints. The “visible–invisible” and “UV–visible” properties of N-CDs promise their applicability in anticounterfeiting. Furthermore, the N-CDs/PVA films with strong and stable emission might find direct or indirect applications in various optical/optoelectronic devices, ranging from fluorescent displays to LEDs.

### ACKNOWLEDGEMENT

Partial financial support comes from the Science Foundation of Sichuan University of Science & Engineering (2020RC06) and the Natural Science Foundation of Sichuan Province (SYZ202133 & 2022JDGD0041). Authors contact email: Jianan Liu: jnLiuad@outlook.com; Chengxiang Wang: 3122532054@qq.com; Rui Zhu: 1299521897@qq.com

### REFERENCES

- [1]. Katharine H, Jennifer F, Zebrafish Get Connected: Investigating Neurotransmission Targets and Alterations in Chemical Toxicity[J].Toxics, 2016, 4(3).
- [2]. Aboulhassan, M. A., et al. "Efficient and sustainable treatment of industrial wastewater using a tannin-based polymer." *International Journal of Sustainable Engineering* 14.6 (2021): 1943-1949.
- [3]. Zamora-Ledezma, Camilo, et al. "Heavy metal water pollution: A fresh look about hazards, novel and conventional remediation methods." *Environmental Technology & Innovation* 22 (2021): 101504.
- [4]. Shellaiah, Muthaiah, and Kien-Wen Sun. "Progress in metal-organic frameworks facilitated mercury detection and removal." *Chemosensors* 9.5 (2021): 101.

- [5]. Wang, Meng, et al. "Dual-ligand lanthanide metal–organic framework probe for ratiometric fluorescence detection of mercury ions in wastewater." *Microchimica Acta* 190.9 (2023): 359.
- [6]. Taneja, Parul, et al. "Detection of cadmium ion in aqueous medium by simultaneous measurement of piezoelectric and electrochemical responses." *Sensors and Actuators B: Chemical* 268 (2018): 144-149.
- [7]. Song, Tao, et al. "Biosorption of cadmium ions from aqueous solution by modified *Auricularia Auricular* matrix waste." *Journal of Molecular Liquids* 241 (2017): 1023-1031.
- [8]. Chen, Jun, et al. "PAAO cryogels from amidoximated P (acrylic acid-co-acrylonitrile) for the adsorption of lead ion." *European Polymer Journal* 171 (2022): 111192.
- [9]. Alnawmasi, Jawza Sh. "Construction of amino-thiol functionalized ion-imprinted chitosan for lead (II) ion removal." *Carbohydrate Polymers* 308 (2023): 120596.
- [10]. Luo, Mao-Ling, et al. "Detection of Arsenic (V) by Fluorescence Sensing Based on Chlorine6-Copper Ion." *Molecules* 29.5 (2024): 1015.
- [11]. Wang, Hongsheng, et al. "Removal of arsenic from aqueous solution using microflower-like  $\delta$ -Bi<sub>2</sub>O<sub>3</sub> as adsorbent: Adsorption characteristics and mechanisms." *Journal of Dispersion Science and Technology* 41.13 (2020): 2026-2036.
- [12]. Bolisetty, Sreenath, Mohammad Peydayesh, and Raffaele Mezzenga. "Sustainable technologies for water purification from heavy metals: review and analysis." *Chemical Society Reviews* 48.2 (2019): 463-487.
- [13]. Gao, Ziyang, et al. "Evolution of the anthropogenic chromium cycle in China." *Journal of Industrial Ecology* 26.2 (2022): 592-608.
- [14]. Shi, *g*, et al. "Formation and immobilization of Cr (VI) species in long-term tannery waste contaminated soils." *Environmental Science & Technology* 54.12 (2020): 7226-7235.
- [15]. Li, Mengna, et al. "Rapid ultrasensitive detection of hexavalent chromium in soil and groundwater by a microProbing imaging platform." *Journal of Hazardous Materials* 433 (2022): 128809.
- [16]. Su *ao*, Su *ao*, et al. "Electrochemically-mediated selective capture of heavy metal chromium and arsenic oxyanions from water." (2018): 4701.
- [17]. Coetzee, Johan J., Neetu Bansal, and Evans MN Chirwa. "Chromium in environment, its toxic effect from chromite-mining and ferrochrome industries, and its possible bioremediation." *Exposure and health* 12 (2020): 51-62.
- [18]. Arancibia, Veronica, et al. "Determination of chromium in urine samples by complexation–supercritical fluid extraction and liquid or gas chromatography." *Journal of Chromatography B* 785.2 (2003): 303-309.
- [19]. Yang, Zhanjun, and Qingchun Lan. "Streptavidin-Functionalized Nitrogen Doped Graphene Platform for Sensitive Electrochemical Immunoassay of Tumor Marker." *Electrochemical Society Meeting Abstracts* 230. No. 52. The Electrochemical Society, Inc., 2016.
- [20]. Anthemidis, Aristidis N., et al. "Flame atomic absorption spectrometric determination of chromium (VI) by on-line preconcentration system using a PTFE packed column." *Talanta* 57.1 (2002): 15-22.
- [21]. Zheng, Min, et al. "On–off–on fluorescent carbon dot nanosensor for recognition of chromium (VI) and ascorbic acid based on the inner filter effect." *ACS applied materials & interfaces* 5.24 (2013): 13242-13247.
- [22]. Pisoschi, Aurelia Magdalena, and Gheorghe Petre Negulescu. "Methods for total antioxidant activity determination: a review." *Biochem Anal Biochem* 1.1 (2011): 106.
- [23]. Shukla, Samiksha, and Mohan Singh Mehata. "Selective picomolar detection of carcinogenic chromium ions using silver nanoparticles capped via biomolecules from flowers of *Plumeria obtusa*." *Journal of Molecular Liquids* 380 (2023): 121705.
- [24]. Jian-feng, Guo, et al. "Colorimetric sensing of chromium (VI) ions in aqueous solution based on the leaching of protein-stabled gold nanoparticles." *Analytical Methods* 8.27 (2016): 5526-5532.
- [25]. Tian, *ao*-Yu, et al. "Highly Sensitive Hydrogel Gratings for Real-Time Detection of Trace Hexavalent Chromium Ions in Water." *Industrial & Engineering Chemistry Research* 62.30 (2023): 11885-11893.
- [26]. Marchesi, Stefano, Chiara Bisio, and Fabio Carniato. "Novel light-emitting clays with structural Tb<sup>3+</sup> and Eu<sup>3+</sup> for chromate anion detection." *RSC advances* 10.50 (2020): 29765-29771.
- [27]. Jain, Shikha, et al. "Boric-acid-functionalized luminescent sensor for detection of chromate ions in aqueous solution." *Materials Letters* 306 (2022): 130933.
- [28]. Ding, Yuxiao, and Zhen - An Qiao. "Carbon surface chemistry: New insight into the old story." *Advanced Materials* 34.42 (2022): 2206025.
- [29]. Y. Jia, L. Zhang, L. Zhuang, H. Liu, X. Yan, X. Wang, J. Liu, J. Wang, Y. Zheng, Z. Xiao, E. Taran, J. Chen, D. Yang, Z. Zhu, S. Wang, L. Dai, X. Yao, Identification of active sites for acidic oxygen reduction on carbon catalysts with and without nitrogen doping, *Nat. Catal.* 2 (2019) 688–695.
- [30]. C. Tang, H.F. Wang, X. Chen, B.Q. Li, T.Z. Hou, B. Zhang, Q. Zhang, M.M. Titirici, F. Wei, Topological defects in metal-free nanocarbon for oxygen electrocatalysis, *Adv. Mater.* 28 (2016) 6845–6851.
- [31]. Y. Jiang, L. Yang, T. Sun, J. Zhao, Z. Lyu, O. Zhuo, X. Wang, Q. Wu, J. Ma, Z. Hu, Significant contribution of intrinsic carbon defects to oxygen reduction activity, *ACS Catal.* 5 (2015) 6707–6712.
- [32]. Y. Jia, L. Zhang, A. Du, G. Gao, J. Chen, X. Yan, C.L. Brown, X. Yao, Defect graphene as a trifunctional catalyst for electrochemical reactions, *Adv. Mater.* 28 (2016) 9532–9538
- [33]. Fu, Zheng, et al. "Utilizing the interfacial reaction of naphthalenyl thiosemicarbazide-modified carbon dots for the ultrasensitive determination of Fe (III) ions." *Spectrochimica Acta Part A: Molecular and Biomolecular Spectroscopy* 225 (2020): 117485.
- [34]. Woo, Jeongyeon, et al. "Green one-pot preparation of carbon dots (CD)-embedded cellulose transparent film for Fe<sup>3+</sup> indicator using ionic liquid." *Cellulose* 27 (2020): 4609-4621.
- [35]. M. Bhatt, S. Bhatt, G. Vyas, I.H. Raval, S. Haldar, P. Paul, Water-dispersible fluorescent carbon dots as bioimaging agents and probes for Hg<sup>2+</sup> and Cu<sup>2+</sup> ions, *ACS Appl Nano Mater.* 3 (7) (2020) 7096–7104.
- [36]. V.D. Dang, A.B. Ganganboina, R.-A. Doang, Bipyridine and copper-functionalized N-doped carbon dots for fluorescence turn off-on detection of ciprofloxacin, *ACS Appl Mater Inter.* 12 (29) (2020) 32247–32258.
- [37]. K.M. Tripathi, T.S. Tran, Y.J. Kim, T. Kim, Green fluorescent onion-like carbon nanoparticles from flaxseed oil for visible light induced photocatalytic applications and label-free detection of Al(III) ions, *ACS Sustain Chem Eng.* 5 (5) (2017) 3982–3992.
- [38]. S. Ahmadian-Fard-Fini, D. Ghanbari, O. Amiri, M. Salavati-Niasari, Electrospinning of cellulose acetate nanofibers/Fe/carbon dot as photoluminescence sensor for mercury(II) and lead(II) ions, *Carbohydr Polym.* 229 (2020) 115428.
- [39]. Bandi, Rajkumar, et al. "Facile conversion of toxic cigarette butts to N, S-codoped carbon dots and their application in fluorescent film, security ink, bioimaging, sensing and logic gate operation." *ACS omega* 3.10 (2018): 13454-13466.
- [40]. Rao, Hanbing, et al. "Smartphone-based fluorescence detection of Al<sup>3+</sup> and H<sub>2</sub>O based on the use of dual-emission biomass carbon dots." *ACS Sustainable Chemistry & Engineering* 8.23 (2020): 8857-8867.
- [41]. Boruah, Anusuya, et al. "Blue-emitting fluorescent carbon quantum dots from waste biomass sources and their application in fluoride ion detection in water." *Journal of Photochemistry and Photobiology B: Biology* 209 (2020): 111940.

- [42]. Quintero-Dallos, V., García-Martínez, J.B., Contreras-Roperero, J.E., Barajas-Ferrerira, C., Barajas-Solano, A.F., Lavecchia, R., Zuorro, A.: Distillery Wastewater as a Sustainable Medium for Microalgae Production 11 (2019): 1526–1533.
- [43]. Tejada, M., García-Martínez, A.M., Parrado, J.: Effects of a vermicompost composted with beet vinasse on soil properties, soil losses and soil restoration. *CATENA* 77 (2009): 238–247
- [44]. Lech, Magdalena, and Karolina Labus. "The methods of brewers' spent grain treatment towards the recovery of valuable ingredients contained therein and comprehensive management of its residues." *Chemical Engineering Research and Design* 183 (2022): 494–511.
- [45]. Nkemaleu, Aurel Thibaut, et al. "Brewery spent grain derived carbon dots for metal sensing." *RSC advances* 12.19 (2022): 11621–11627.
- [46]. Kazak, Omer, et al. "Preparation of chemically-activated high surface area carbon from waste vinasse and its efficiency as adsorbent material." *Journal of Molecular Liquids* 272 (2018): 189–197.
- [47]. Chen, Chao, et al. "An effective pre-burning treatment boosting adsorption capacity of sorghum distillers' grain derived porous carbon." *Diamond and Related Materials* 124 (2022): 108914.
- [48]. Miao, X.; Yan, X.; Qu, D.; Li, D.; Tao, F. F.; Sun, Z. Red Emissive Sulfur, Nitrogen Codoped Carbon Dots and Their Application in Ion Detection and Theranostics. *ACS Appl. Mater. Interfaces* 9 (2017), 18549–18556.
- [49]. X. Geng, Y. Sun, Z. Li, R. Yang, Y. Zhao, Y. Guo, J. Xu, F. Li, Y. Wang, S. Lu, L. Qu, Retrosynthesis of tunable fluorescent carbon dots for precise long-term mitochondrial tracking, *Small* 15 (2019) 1901517.
- [50]. Gao, Dong, et al. "Temperature triggered high-performance carbon dots with robust solvatochromic effect and self-quenching-resistant deep red solid state fluorescence for specific lipid droplet imaging." *Chemical Engineering Journal* 415 (2021): 128984.
- [51]. Xu, Quan, et al. "Recent progress of quantum dots for energy storage applications." *Carbon Neutrality* 1.1 (2022): 13.
- [52]. Ding, S.-B. Yu, J.-S. Wei, H.-M. Xiong, Full-color light-emitting carbon dots with a surface-state-controlled luminescence mechanism, *ACS Nano* 10 (2016) 484–491.
- [53]. Li, Weidong, et al. "Carbon - quantum - dots - loaded ruthenium nanoparticles as an efficient electrocatalyst for hydrogen production in alkaline media." *Advanced Materials* 30.31 (2018): 1800676.
- [54]. Chen, Weifeng, et al. "Catalyzed hydrolysis of tetrahydroxydiboron by graphene quantum dot-stabilized transition-metal nanoparticles for hydrogen evolution." *ACS Sustainable Chemistry & Engineering* 8.19 (2020): 7513-7522.
- [55]. Lv, P. F.; Yao, Y. X.; Zhou, H. M.; Zhang, J.; Pang, Z. Y.; Ao, K. L.; Cai, Y. B.; Wei, Q. F. Synthesis of novel nitrogen-doped carbon dots for highly selective detection of iron ion. *Nanotechnology* 28 (2017), No. 165502.
- [56]. Shen, Jialu, et al. "Wattle-Bark-Tannin-Derived Carbon Quantum Dots as Multi-Functional Nanomaterials for Intelligent Detection of Cr<sup>6+</sup> Ions, Bio-Imaging, and Fluorescent Ink Applications." *Industrial & Engineering Chemistry Research* 62.8 (2023): 3622-3634.
- [57]. \*\*e, Hai-Fang, et al. "7RX, UK.† Footnotes relating to the title and/or authors should appear here. Electronic Supplementary Information (ESI) available: 1H/13C NMR spectra and the absorption spectra of probe, etc. See DOI: 10.1039/x0xx00000x. School of Public Health, the key Laboratory of Environmental Pollution Monitoring and Disease Control."
- [58]. Wei, Shanshan, et al. "Portable smartphone platform based on tunable chiral fluorescent carbon dots for visual detection of L-Asp and L-Lys." *Chemical Engineering Journal* 466 (2023): 143103.
- [59]. Yuan, Kang, et al. "Surface state modulation of red emitting carbon dots for white light-emitting diodes." *Journal of Materials Chemistry C* 6.46 (2018): 12631-12637.
- [60]. Zhang, Yuhua, et al. "Optimization of ionic liquid-mediated red-emission carbon dots and their imaging application in living cells." *ACS Sustainable Chemistry & Engineering* 8.45 (2020): 16979-16989.
- [61]. Liu, Junjun, et al. "Deep red emissive carbonized polymer dots with unprecedented narrow full width at half maximum." *Advanced materials* 32.17 (2020): 1906641.
- [62]. Hu, Lulu, et al. "Nitrogen and sulfur co-doped chiral carbon quantum dots with independent photoluminescence and chirality." *Inorganic Chemistry Frontiers* 4.6 (2017): 946-953.
- [63]. Ramanan, Vadivel, et al. "Green synthesis of multifunctionalized, nitrogen-doped, highly fluorescent carbon dots from waste expanded polystyrene and its application in the fluorimetric detection of Au<sup>3+</sup> ions in aqueous media." *ACS Sustainable Chemistry & Engineering* 6.2 (2018): 1627-1638.
- [64]. Van Dam, Bart, et al. "Excitation - dependent photoluminescence from single - carbon dots." *Small* 13.48 (2017): 1702098.
- [65]. Feng, Mi, et al. "Chitin-based carbon dots with tunable photoluminescence for Fe<sup>3+</sup> detection." *ACS Applied Nano Materials* 5.5 (2022): 7502-7511.
- [66]. Zheng, Min, et al. "On-off-on fluorescent carbon dot nanosensor for recognition of chromium (VI) and ascorbic acid based on the inner filter effect." *ACS applied materials & interfaces* 5.24 (2013): 13242-13247.
- [67]. Xu, \*\*ang - Rong, et al. "Kinetics of the reduction of chromium (VI) by vitamin C." *Environmental Toxicology and Chemistry: An International Journal* 24.6 (2005): 1310-1314.
- [68]. Dhal, B., et al. "Chemical and microbial remediation of hexavalent chromium from contaminated soil and mining/metallurgical solid waste: a review." *Journal of hazardous materials* 250 (2013): 272-291.
- [69]. Lu, Wen\*\*g, et al. "High-quality water-soluble luminescent carbon dots for multicolor patterning, sensors, and bioimaging." *RSC Advances* 5.22 (2015): 16972-16979.
- [70]. Kwan, Melvin Ng Hau, et al. "Carbon-dot dispersal in PVA thin film for food colorant sensing." *Journal of Environmental Chemical Engineering* 8.3 (2020): 103187.